

25 Oct 2020

## Thermo-coupled Temperature Sensors By Seven-core MCF Structures

Farhan Mumtaz

Missouri University of Science and Technology, mfmawan@mst.edu

Yutang Dai

Wenbin Hu

Muhammad Aqueel Ashraf

*et. al.* For a complete list of authors, see [https://scholarsmine.mst.edu/ele\\_comeng\\_facwork/5069](https://scholarsmine.mst.edu/ele_comeng_facwork/5069)

Follow this and additional works at: [https://scholarsmine.mst.edu/ele\\_comeng\\_facwork](https://scholarsmine.mst.edu/ele_comeng_facwork)

 Part of the [Electrical and Computer Engineering Commons](#)

---

### Recommended Citation

F. Mumtaz et al., "Thermo-coupled Temperature Sensors By Seven-core MCF Structures," *Proceedings of IEEE Sensors*, article no. 9278856, Institute of Electrical and Electronics Engineers, Oct 2020.

The definitive version is available at <https://doi.org/10.1109/SENSORS47125.2020.9278856>

This Article - Conference proceedings is brought to you for free and open access by Scholars' Mine. It has been accepted for inclusion in Electrical and Computer Engineering Faculty Research & Creative Works by an authorized administrator of Scholars' Mine. This work is protected by U. S. Copyright Law. Unauthorized use including reproduction for redistribution requires the permission of the copyright holder. For more information, please contact [scholarsmine@mst.edu](mailto:scholarsmine@mst.edu).

# Thermo-coupled Temperature Sensors by seven-core MCF Structures

Farhan Mumtaz<sup>1,2,3</sup>, Yutang Dai<sup>1\*</sup>, Wenbin Hu<sup>1\*</sup>, Muhammad Aqueel Ashraf<sup>3</sup>, Shu Cheng<sup>1</sup>, Pu Cheng<sup>1</sup>

<sup>1</sup> National Engineering Laboratory for Fibre Optic Sensing Technology, Wuhan University of Technology, Wuhan 430070, China.

<sup>2</sup> School of Information and Communication Engineering, Wuhan University of Technology, China.

<sup>3</sup> Communications Lab. Department of Electronics, Quaid-i-Azam University, Islamabad, 45320, Pakistan.

[mfmawan@whut.edu.cn](mailto:mfmawan@whut.edu.cn) (F. Mumtaz), [\\*daiyt6688@whut.edu.cn](mailto:*daiyt6688@whut.edu.cn) (Y. Dai), [\\*wenbinhu\\_whut@163.com](mailto:*wenbinhu_whut@163.com) (W. Hu), [aqueel@qau.edu.pk](mailto:aqueel@qau.edu.pk) (M.A. Ashraf)

**Abstract**— In this paper, we present an enhanced sensitivity of temperature sensors based on thermo-coupled Multicore Fiber (MCF) structures. The sensors are all fabricated using a controlled arc power of a splicing device. Two different principles of a Mach-Zehnder interferometer (MZI) and Michelson interferometer (MI) have been observed experimentally. The MZI and MI structures exhibit temperature sensitivity as 136.67 pm/°C and 70.61 pm/°C, respectively, and found insensitive to the refractive index (RI). Also, its RI response can readily resolve the issues of cross-sensitivity.

**Keywords**— Multi-core optical Fiber; Thermo-coupled temperature sensors.

## I. INTRODUCTION

In the field of optical sensing, MCF has set a new paradigm of innovation. In-addition, MCF constitutes a viable platform for testing various physical quantities, such as refractive index (RI), temperature, strain, curvature and etc. By means of MCF [1]-[3], various applications have been developed in the field of biology, medicine and chemical. Although it is reliable and compatible with multiple devices and can be easily embedded in MZI [4]-[6] and MI [7]-[9] configurations. The interference from the outer cores of MCF makes an interferometer highly sensitive to the environment. In addition to the structures based on a tapered MCF and single-mode fiber (SMF) lead-in/out [10], the proposed structure based on ellipsoidal balls (EB) in-line MCF can also effectively produce an interference spectrum.

An effort is made to fabricate two different principles of temperature sensors based on MCF. The MZI and MI are fabricated by creating EB in the interferometer structures. The MCF of seven cores is used, a center and six hexagonal distributed outer cores. When the external temperature rises, then a thermo-coupling effect of MCF can be realized. Such effects tend to produce a shift in wavelength and also improve the sensitivity of an interferometer. The proposed sensors have substantially enhanced the temperature sensitivity by two to four times as compared with SMF [11] and multimode fibers (MMF) [12] structures, whereas the SMF and MMF structures exhibit sensitivity of 26.03 pm/°C, 49 pm/°C, respectively. In-addition, our sensors offer ten times better sensitivity than a Fibre Bragg gratings (FBG) [13], whereas FBG shown the maximum sensitivity of 10 - 13 pm/°C. Also, the sensors have

revealed the merits of simple fabrication, stable response, reproducible, non-fragile, highly sensitive, and nil cross-sensitivity.

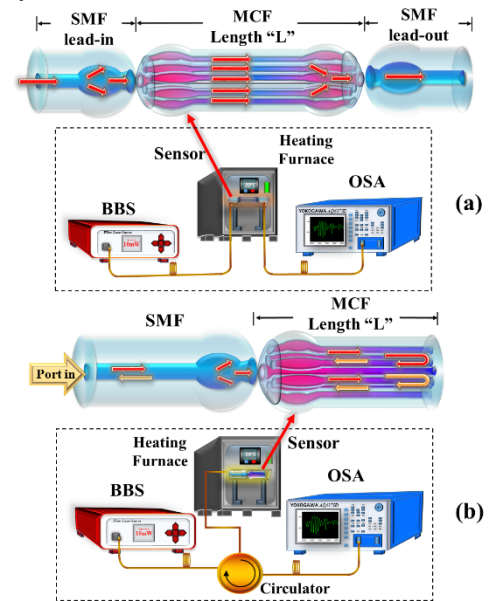


**Fig. 1.** (a) SMS~MZI and (b) MCF~MI and their experimental setup for temperature measurement

## II. WORKING PRINCIPLE

The schematic diagram of the proposed thermo-coupled SMS~MZI (SMF-MCF-SMF~MZI) and SM~MI (SMF-MCF~MI) temperature sensors, and their corresponding experimental setups are shown in Fig. 1(a) and Fig. 1(b), respectively. Equally all of the structures are fabricated using a controlled arc power of a commercial splicer (Furukawa Fitel S177). An optical spectrum analyzer (OSA) is employed in the experiments to monitor the wavelength shift with temperature variations. The deployment of EB in the proposed SMS~MZI and SM~MI sensors have significantly enhanced the interference. The cladding and outer core modes of MCF are excited when the light intensity entered from the first EB junction. The interference occurs due to the optical path difference between two distinct beams of light intensity, and total intensity of interferometer at the output can be expressed as,

$$I_{total} = I_c + I_s + 2\sqrt{I_c I_s} \cos(\varphi + \varphi_0) \quad (1)$$

where  $\varphi_0$  is the initial phase and  $\varphi$  is the phase difference between two super-modes carried by  $I_c$  and  $I_s$ , respectively.

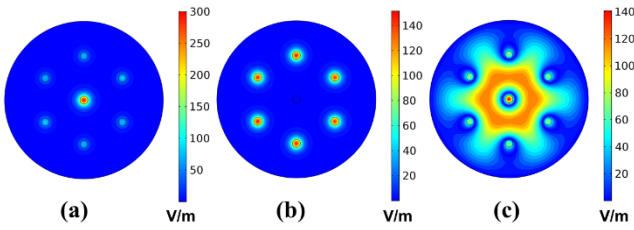


**Fig. 2.** Transverse Electric field profiles of super-mode associated with the (a) center core, (b) side cores, and (c) cladding mode.

For the SMS~MZI, the light intensities carried by the super-modes are coupled at first EB junction and re-coupled back at the second EB junction. Each junction is made up of the pair of EB as shown in Fig. 1(a). Thus the phase difference for the SMS~MZI can be expressed as,

$$\varphi = \frac{2\pi\Delta n_{eff}^{c,s}L}{\lambda_{mzi}} \quad (2)$$

Whereas the SM~MI sensor is constituted by a MI principle. As the light coming from the SMF core is entered through EB junction and then spreads into the cladding and outer cores of MCF. The light propagates in the MCF, is then reflected back from the end face of MCF, as shown in Fig. 1(b). Thus the phase difference for SM~MI can be expressed as,

$$\varphi = \frac{4\pi\Delta n_{eff}^{c,s}L}{\lambda_{mi}} \quad (3)$$

where,  $\lambda_{mzi}$  and  $\lambda_{mi}$  are the operating wavelengths,  $\Delta n_{eff}^{c,s}$  is the relative effective refractive index difference between the center core and outer core modes, and  $L$  is a MCF length.

When the effective refractive index difference of the  $m^{th}$ -order interference dip will shift with the change of the ambient temperature. Then, the relation of temperature sensitivity for a SMS~MZI sensor can be estimated as [4],

$$\frac{d\lambda_{mzi}}{dT} = \frac{\lambda_{mzi}}{\Delta n_{eff}^{c,s}} \left[ \frac{dn_{eff}^c}{dT} - \frac{dn_{eff}^s}{dT} \right] \quad (4)$$

and after that, the temperature sensitivity for a SM~MI sensor can be estimated as [8],

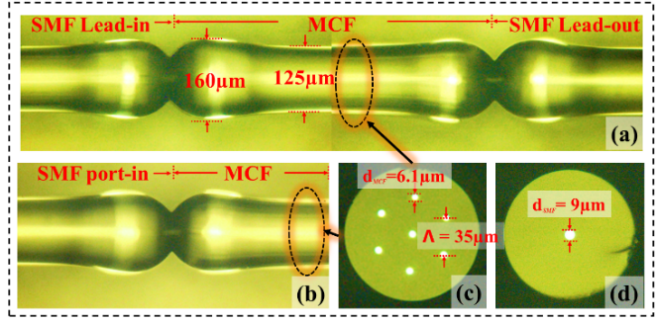
$$\frac{d\lambda_{mi}}{dT} = 2\lambda_{mi} \left[ \frac{1}{\Delta n_{eff}^{c,s}} \left( \frac{dn_{eff}^c}{dT} - \frac{dn_{eff}^s}{dT} \right) + \frac{1}{L} \left( \frac{dL}{dT} \right) \right] \quad (5)$$

TABLE I. FIBER PARAMETERS

Fibre Type	Diameter ( $\mu\text{m}$ )		Refractive index		$\Lambda$ Pitch ( $\mu\text{m}$ )
	Core	Clad	Core	Clad	
SMF	9	125	1.462	1.457	NIL
MCF	6.1	125	1.4681	1.4628	35

When light is launched from SMF Lead-in, several higher-order modes are excited as the light passes through EB junction. Most of them will degenerate in intensity due to different phases across the MCF cores. The input SMF light intensity can allow only two dominant super-modes to propagate in MCF. Whereas such modes can be generated with the assistance of cladding mode. Here, cladding mode will act as a facilitator of two dominated super-modes while propagates through the MCF. The simulated Electric field plots of such super-mode modes are obtained by the COMSOL, which are associated with the center core, outer

cores, and cladding mode, as shown in Fig. 2(a-c), respectively.



**Fig. 3.** Sensors under the microscope; longitudinal cross-section of (a) SMS~MZI, (b) SM~MI, and transverse cross-section of (c) MCF. (d) SMF.

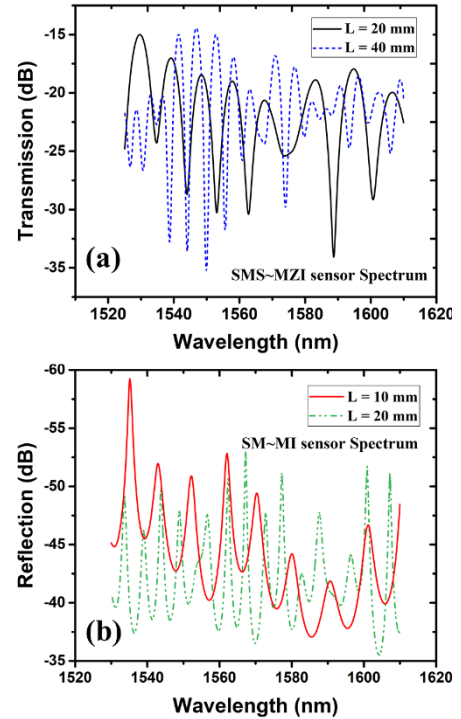


**Fig. 4.** Interference spectrum of (a) SMS~MZI, and (b) SM~MI sensors

### III. FABRICATION AND INTERFERENCE SPECTRUM

The MCF (FIBRECORE, SM-7C1500) is used as the sensing element in our proposed SMS~MZI and SM~MI structures. The sensors can be fabricated the following steps. First of all, the cleaved end face of SMF and MCF were individually fused using a controlled arc power of +100 bits with a run time of 750 ms of a splicer, so that EB could be formed. The constituted EBs were symmetrical and had 160  $\mu\text{m}$  diameter at mid-section. Whereas the original diameter of SMF and MCF was 125  $\mu\text{m}$ . Afterward, these EB were spliced together using a normal arc power of multimode function in the splicer menu. Then, the above procedure was repeated, so that another analogous set of EB was formed at a distance  $L$  from the first EB, and SMS~MZI could be fabricated, as shown in Fig. 3(a). Whereas, SMS~MI was required only one set of EB, so we were cleaved the MCF at a distance of  $L$  from an EB. Thus the SMS~MI was fabricated, as shown in Fig. 3(b). The transverse cross-section of utilized fibers under the microscope can be seen in Fig. 3(c-d).

In our experiment, two different  $L$  of each sensor were used to measure the temperature response. The core and clad parameters of utilized fibers are listed in the Table. 1

The interference spectrum of the SMS~MZI and SM~MI was measured with two different experimental setups, as shown in Fig. 1(a) and Fig. 1(b), respectively. A broadband light source (BBS) was used as light sources with a flat frequency band range from 1520 nm to 1610 nm. The transmission and reflection spectrum was detected using an OSA with a spectral resolution of 0.02 nm. In order to determine the number and power distribution of modes, the interference spectra of the SMS~MZI and SM~MI sensors were independently obtained, as shown in Fig. 4(a) and Fig. 4(b), respectively.

#### IV. EXPERIMENT AND DISCUSSION

In order to measure the temperature and RI responses, two different experimental setups are considered for SMS~MZI and SMS~MI, which are as follow:

##### A. SMS~MZI temperature response

The schematic experimental setup of SMS~MZI is shown in Fig. 1(a). The sensors were placed into the temperature furnace with a temperature error of  $\pm 0.01^\circ\text{C}$ , approximately. The internal temperature of the apparatus was kept for 20 mins during each heating process. Two different “ $L = 20\text{ mm} \& 40\text{ mm}$ ” of SMS~MZI sensors were employed one after the other. In the response of temperature rose, the interference dips were significantly shifted toward a longer wavelength, and produced a red-shift in the range of  $20^\circ\text{C}$  to  $90^\circ\text{C}$ . The SMS~MZI sensors of “ $L = 20\text{ mm} \& 40\text{ mm}$ ” have displayed a higher temperature sensitivity of  $68.27\text{ pm}/^\circ\text{C}$  and  $136.67\text{ pm}/^\circ\text{C}$  with a good linearity response of 0.995 and 0.991, respectively, as shown in Fig. 5. The temperature sensitivity of proposed SMS~MZI is found better than reported MZI interferometers based on MCF in [5] and [6], whereas these MZI showed sensitivity of  $76\text{ pm}/^\circ\text{C}$  and  $82\text{ pm}/^\circ\text{C}$  respectively.

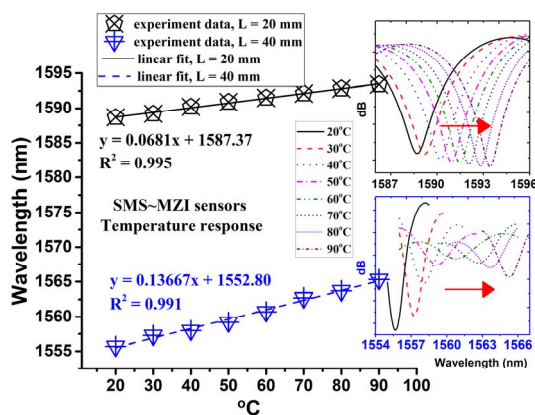


Fig. 5. SMS~MZI sensors temperature sensitivity and linearity response, and inset of wavelength shift with temperature rose.

##### B. SM~MI temperature response

Later, the SM~MI sensors were tested with another experimental setup, as shown in Fig. 1(b). Likewise, by using the aforementioned procedure, these sensors were examined for temperature responses. Here also, two different “ $L = 10\text{ mm} \& 20\text{ mm}$ ” of SM~MI sensors were employed one after the other. In the response of external temperature rose, the interference dips of SM~MI sensors had also produced a red-shift in the range of  $20^\circ\text{C}$  to  $90^\circ\text{C}$ . The SM~MI sensors of “ $L = 10\text{ mm} \& 20\text{ mm}$ ” have displayed a

higher temperature sensitivity of  $65.10\text{ pm}/^\circ\text{C}$  and  $70.61\text{ pm}/^\circ\text{C}$  with a good linearity response of 0.999 and 0.996, respectively, as shown in Fig. 6. Also SMS~MI structure exhibits superior sensitivity than the reported MI interferometer based on MCF [7], and presented sensitivity of  $40\text{ pm}/^\circ\text{C}$  in the range of  $0\text{--}200^\circ\text{C}$ .

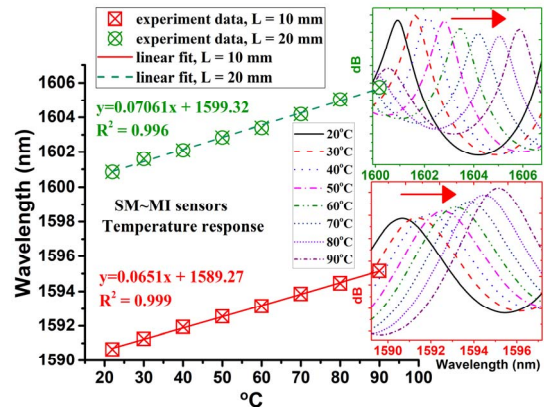


Fig. 6. SM~MI sensors temperature sensitivity and linearity response, and inset of wavelength shift with temperature rose.

Besides, we have experimentally demonstrated the RI responses of SMS~MZI and SM~MI sensors. The sensors were found to be insensitive in the range of 1.333 to 1.354. It can be observed that a very small fluctuation of interference dips was seen when external RI was changed. The fluctuation might be intervened due to the slight temperature difference of employed NaCl solution. Whereas, it was not affected by the change in external RI. The insensitive RI response and dips experimental data are shown in Fig. 7.

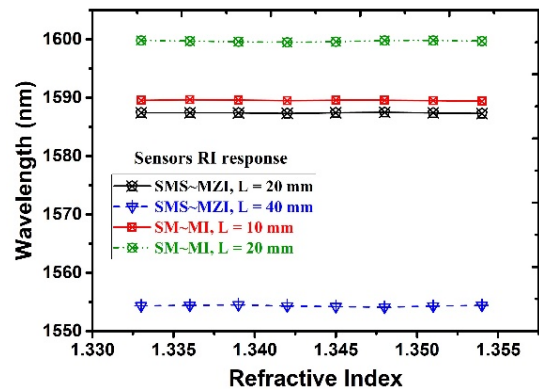


Fig. 7. The sensors respond to the surrounding refractive index.

#### V. CONCLUSION

In conclusion, two different principles of temperature sensors based on thermo-coupled MCF structures are presented. The use of EB configuration in SMS~MZI and SM~MI structures has significantly improved sensitivity and interference strength. The sensors are well elucidated that such structures can be part of sea-water and biological applications. Besides, such structures will also address the challenges of cross-sensitivity.

#### ACKNOWLEDGMENT

This work was supported in part by the Major Technique Innovation Program of Hubei Province of China under Grant 2018AAA016, in part by the National Key Research and Development Program of China under Grant 2017YFB0405501, and in part by the National Natural Science Foundation of China under Grant 51975442.

## REFERENCES

- [1] Libo Yuan "Recent progress of multi-core fiber based integrated interferometers", Proc. SPIE 7508, 2009 International Conference on Optical Instruments and Technology: Advanced Sensor Technologies and Applications, 750802 (23 November 2009); <https://doi.org/10.1117/12.837912>
- [2] F. Mumtaz, Y. Dai and M. A. Ashraf, "Inter-cross de-modulated refractive index and temperature sensor by an etched Multi-core fiber of a MZI structure," in *Journal of Lightwave Technology*, doi: 10.1109/JLT.2020.3014857.
- [3] Paul S. Westbrook, K. S. Feder, T. Kremp, T. F. Taunay, E. Monberg, G. Puc, and R. Ortiz "Multicore optical fiber grating array fabrication for medical sensing applications", Proc. SPIE 9317, Optical Fibers and Sensors for Medical Diagnostics and Treatment Applications XV, 93170C (5 March 2015); <https://doi.org/10.1117/12.2077833>
- [4] Mumtaz F, Cheng P, Li C, Cheng S, Du C, Yang M, Dai Y, Hu W., "A design of taper-like etched multicore fiber refractive index-insensitive a temperature highly sensitive Mach-Zehnder interferometer", *IEEE Sensors Journal*, vol. 20, no. 13, pp. 7074-7081, July. 2020.
- [5] Li, H., Li, H., Meng, F., Lou, X. and Zhu, L., "All-fiber MZI sensor based on seven-core fiber and fiber ball symmetrical structure", *Optics and Lasers in Engineering*, vol. 112, pp. 1-6, 2019.
- [6] Jiang, Y., Wang, T., Liu, C., Feng, D., Jiang, B., Yang, D. and Zhao, J., "Simultaneous measurement of refractive index and temperature with high sensitivity based on a multipath fiber Mach-Zehnder interferometer," *Appl. Opt.* vol. 58, no. 15, pp. 4085-40, 2019
- [7] Duan L, Zhang P, Tang M, Wang R, Zhao Z, Fu S, Gan L, Zhu B, Tong W, Liu D, Shum PP. Heterogeneous all-solid multicore fiber based multipath Michelson interferometer for high temperature sensing. *Optics express*. vol. 24, no. 18, pp. 20210-8, Sep. 2016.
- [8] Wu D, Zhu T, Liu M. "A high temperature sensor based on a peanut-shape structure Michelson interferometer", *Optics Communications*, vol. 285, no. 24, pp: 5085-8, Nov. 2012.
- [9] Zhou A, Zhang Y, Li G, Yang J, Wang Y, Tian F, Yuan L. "Optical refractometer based on an asymmetrical twin-core fiber Michelson interferometer", *Optics Letters*, vol. 36, no.16: pp. 3221-3223, 2011.
- [10] Cheng P, Yang M, Hu W, Guo D, Du C, Luo X, Mumtaz F., "Refractive index interferometer based on SMF-MMF-TMCF-SMF structure with low temperature sensitivity". *Optical Fiber Technology*. vol. 57, pp:102233, Jul. 2020.
- [11] Tan J, Feng G, Liang J, Zhang S., "Optical fiber temperature sensor based on dumbbell-shaped Mach-Zehnder interferometer", *Optical Engineering*.; vol. 57, no. 1, pp :017112, Jan. 2018.
- [12] Rui Xing, Changbin Dong, Zixiao Wang, Yue Wu, Yuguang Yang, Shuisheng Jian, "Simultaneous strain and temperature sensor based on polarization maintaining fiber and multimode fiber", *Opt. Laser Technol.* vol. 102 ,pp: 17-21, Jun. 2018.
- [13] Y. J. Rao, "In-fibre Bragg grating sensors", *Meas. Sci. Technol.*, vol. 8, pp. 355-375, Apr. 1997.